Sensitivity of WRF-HAILCAST Model for Hailstone Detection in Central Lombok on 24 February 2019

Muhammad Ikko Safrilda Maulana[1] and Aries Kristianto[2]

[1]*Soekarno Hatta Meteorological Station, Bandara Soekarno Hatta, Gedung 725, Kota Tangerang, 15125*
[2]*Meteorology, Sekolah Tinggi Meteorologi Klimatologi dan Geofisika, Jl. Perhubungan I No. 5, Kota Tangerang Selatan, 15221*

Abstract: Hail is a type of extreme weather produced by Cumulonimbus clouds or convective clouds. Due to deep convection involve in physical processes and cloud dynamics, hail may occur in Indonesia. WRF-HAILCAST was used in this study to detect hailstone. The HAILCAST model is applied to WRF-ARW version 4.0 and above in WRF-HAILCAST. The purpose of this study was to determine the sensitivity of the WRF-HAILCAST model with a modified WSM6 microphysics scheme to detect hailstones that are possible to reach the surface. The maximum reflectivity value, vertical reflectivity, maximum hailstone diameter, and cloud microphysics were all approximated properly as a result of this study. The estimation of the maximum diameter hailstone was 1.6 cm at the time of hail occurred, and the graupel mixing ratio showed 2.2 g/kg which represented small hail could be detected in this model. However, WRF-HAILCAST tends to underestimate and has not been able to estimate the time of hail events according to weather radar properly. This research can contribute to hailstone detection in Indonesia using numerical methods and give a breakthrough in hailstone detection and disaster preparedness.

Keywords: Hailstone size; microphysics scheme; verification; WRF-HAILCAST

*Corresponding author: maulanaikko@gmail.com

http://dx.doi.org/10.12962/j24604682.v20i1.14010
2460-4682

I. INTRODUCTION

Extreme weather is a rare and exceptional weather occurrence that has the potential to cause property damage and human fatalities [1]. In terms of cloud physics, hail can be produced by supersaturation of the air with liquid water, which results in the formation of clouds also called the condensation process. The control factor for the mass growth of ice crystals occurs through heterogeneous deposition in the atmosphere when ice crystals are concentrated in clouds during the collision and coalescence mechanism with other ice crystals. Heterogeneous deposition can occur if there are condensation nuclei in the cloud. The condensation nuclei can contribute to the sticking ice crystal during the collision and coalescence process. During those processes, it will contribute to the increase in mass and particle size so that it becomes denser which is called a hailstone. If there is a downdraft in the cloud and it is supported by a relatively cold surface temperature, the hailstone will be lifted above the freezing level so that when it reaches the surface the hailstone does not melt completely and hail fall can occur [2]. Hail is an uncommon event in the tropics because of relatively cold temperatures on the surface, but deep convection with intense updrafts and downdrafts occurs frequently [3]. Hail in the tropics is conceivable due to the effects of updraft and downdraft in storm clouds, which can rapidly drop hailstone in the clouds to the surface. Hail is another local occurrence that is difficult to predict, uneven, and occurs unexpectedly [4]. Hailstone detection using weather radar in Indonesia is a very common method, but this research gives a breakthrough to detect hailstone using a numerical model. The importance of hail detection in Indonesia can be applied for weather forecasting and disaster preparedness although the hail occurrence is very rare in this region.

HAILCAST combines a time-dependent hail growth model with a one-dimensional cloud steady-state model [5]. HAILCAST calculates atmospheric profiles such as temperature, humidity, and wind used to drive cloud models and generates simulated vertical profiles with vertical velocity, liquid water and ice content, and temperature associated with the cloud [6]. Large-scale circulation, dominant hydrometeor fields, and processes associated with storm systems or convective systems can be generated by the HAILCAST model when run at a spatial resolution of 4 km or finer [7, 8]. Tests of the WRF-HAILCAST model have been carried out by [6] which resulted in realistic predictions of hail prediction without any modification at a spatial resolution of 1 km. The HAILCAST model from [9] and [5] has been significantly improved in this WRF-ARW hereinafter referred to as WRF-HAILCAST.

According to information from Detik.com, there was a hail occurrence on February 24, 2019, in Tapon Barat, Bilebante, Pringgarata District, Central Lombok, and West Nusa Tenggara. Around 8:00 UTC, this event happens after a period of severe rain. The WRF-HAILCAST model was expected to give an output that is capable of producing an accurate hail simulation in terms of atmospheric conditions in Central Lombok on February 24, 2019 at 04.00 12.00 UTC by using the best microphysical parameterization scheme from the prior research in [10].

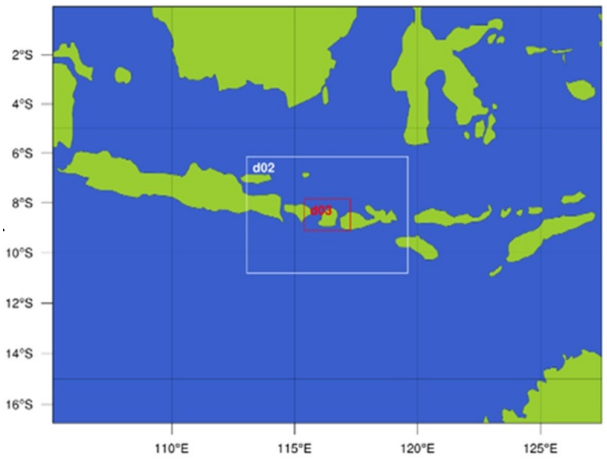

FIG. 1: Domain configuration of WRF-HAILCAST

II. METHODOLOGY

The WRF-HAILCAST model is used to detect hailstones on February 24, 2019 between 4:00-12:00 UTC, with Final Analysis (FNL) reanalysis data used as the model's initial condition. These data were obtained in .grib2 format from the https://rda.ucar.edu/ site. Data from FNL reanalysis has a resolution of 0.25 and a temporal resolution of 6 hours. The length of data was at 00, 06, and 12 UTC.

The Lombok Meteorological Station provides weather radar data every 10 minutes from 07:00 to 20:00 UTC. The CMAX product which shows the radar's highest reflectivity value, and the VCUT product, which shows a vertical slice of the storm cloud structure, were both used in this study [11]. The threshold reflectivity from [9] of 52 dBZ and the threshold of freezing level from [12] of 5 km are utilized to determine the probability of hail. Additionally, the analysis of cloud microphysics variables that made up mixing ratio of hydrometeor particles, which include vapor, cloud water, rain, ice, and graupel.

In this study, three domains were Domain 1 with a resolution of 24.3 km, Domain 2 with a resolution of 8.1 km, and Domain 3 with a resolution of 2.7 km, as summarized in Table I. Those domains were used in the nesting process of WRF-HAILCAST. Nevertheless, only Domain 3 was examined in this study because it possessed the finest resolution out of the three. Additionally, the WSM6 microphysics scheme was chosen based on an earlier study by [10] that was the best microphysics scheme.

The next process was post-processing, it used ARWpost and GrADS software. ARWpost converted the WRF-HAILCAST output and GrADS was used to display the variables in this study. To determine the sensitivity of the model, hereinafter the verification model used several methods that are Root Mean Square Error (RMSE), Pearson Coefficient, Mean Bias Error, and visual verification. Microsoft Excel 2016 was used to calculate those methods.

TABLE I: Configuration of WRF-HAILCAST

Parameterization Schemes	(Domain 1)	(Domain 2)	(Domain 3)
Resolution (km)	24.3	8.1	2.7
Microphysics		WSM6	
Cumulus		No Cumulus	
Longwave radiation		RRTM	
Shortwave radiation		Dudhia	
Planetary Boundary Layer		YSU	
Surface		NOAH	

TABLE II: Correlation Coefficient Category

Interval	Correlation Rate
0.00 - 0.199	Very weak
0.20 - 0.399	Weak
0.40 - 0.599	Moderate
0.60 - 0.799	Strong
0.80 - 1.000	Very Strong

A. Root Mean Square Error (RMSE)

RMSE describes the average magnitude of errors, it calculates based on the square of the error. The larger magnitude of RMSE indicates a larger error. Its sensitivity to large errors means that the model may not give stable estimates of error [13]. The RMSE equation is shown as follows.

$$RMSE = \sqrt{\frac{\Sigma_{i=1}^{n}(F_i - O_i)^2}{n}} \quad (1)$$

with n = lots of data, F_i = the value of the i-th WRF model output variable, O_i = the value of the i-th observation variable.

B. Pearson Correlation

Pearson Correlation is a number that states the level of the relationship between two variables [14]. It ranges from -1 to 1. Table II shows the categories of Pearson Correlation. Pearson Correlation equation is shown as follows.

$$C = \frac{\Sigma_{i=1}^{n}(FO)(F_i - \vec{F})}{\sqrt{\Sigma_{i=1}^{n}(O_i - \vec{O})^2}\sqrt{\Sigma_{i=1}^{n}(Fi - \vec{F})^2}} \quad (2)$$

with a value of n = lots of data, $\vec{F}$ = average of WRF model output variable data, $\vec{O}$ = average of observational variable data, F_i = i-th value of WRF model output variable, O_i = i-th value of an observational variable.

C. Mean Bias Error (MBE)

MBE defines a model's average bias as the systematic inaccuracy that results in estimations that are both underestimate

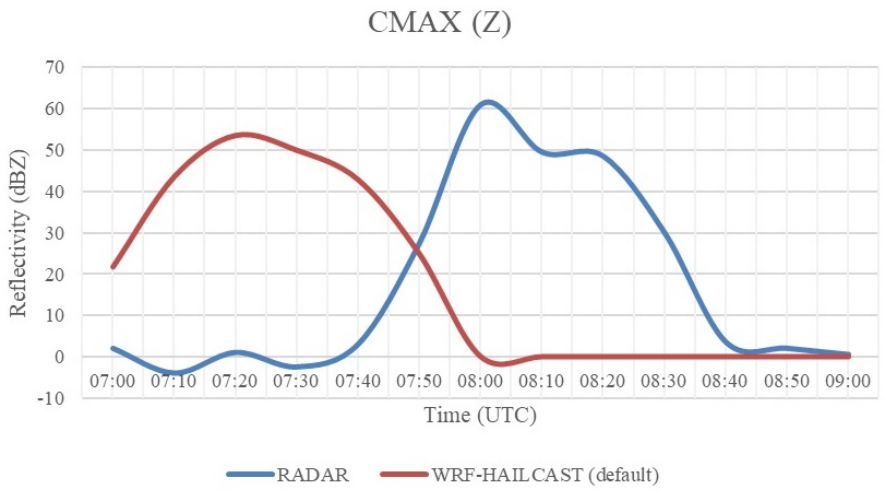

FIG. 2: Time series of radar maximum reflectivity and WRF-HAILCAST

and overestimate. A tendency to exaggerate the observational data is indicated by a positive value. Additionally, a negative value denotes a tendency to underestimate the observation [15]. The MBE equation is shown as follows.

$$MBE = \frac{1}{n}\Sigma_{i=1}^{n}(F_i - O_i) \quad (3)$$

with n = lots of data, F_i = the value of the i-th WRF model output variable, and O_i = the value of the i-th observation variable.

D. Visual Verification

The best approach for validating the outcomes of the visual image of the model output is visual verification, which is the oldest method [16]. To determine the accuracy of the model estimate, this method compares the outcomes of model estimation with observations while employing human judgment. The analysis of time series and spatial descriptions of model output variables can be done using this technique.

III. RESULTS AND DISCUSSIONS

A. WRF-HAILCAST Model Verification to CMAX Radar Reflectivity Data

Verification is carried out by comparing the output of the WRF-HAILCAST model and the Lombok Weather Radar observation data located at coordinates -8.636S; 116,171E. Table III shows the results of calculating the RMSE value, Pearson Correlation, and Mean Bias Error (MBE). This verification process is carried out every 10 minutes starting at 07.00-09.00 UTC.

Based on Table III, the RMSE value is 38.45 and the correlation coefficient shows a moderate level of negative relation. While the MBE value shows a tendency to underestimate

TABLE III: Verification of WRF-HAILCAST model output to CMAX Radar

TIME (UTC)	RADAR	WRF-HAILCAST (default)	Bias Error-i
07:00	2	22	-20
07:10	-4	44	-48
07:20	1	54	-53
07:30	-3	50	-53
07:40	3	43	-40
07:50	28	25	3
08:00	61	0	61
08:10	50	0	50
08:20	49	0	49
08:30	30	0	30
08:40	3.5	0	4
08:50	2	0	2
09:00	1	0	1
RMSE		38.45	
Pearson Correlation		-0.56	
MBE		-1.13	

the estimated reflectivity value. Negative correlation indicates that the model shows the negative relation between radar and WRF-HAILCAST model. When viewed from the maximum reflectivity value from the radar, it shows a maximum value of 61 dBZ which interprets the occurrence of hail. While the estimated maximum reflectivity value of the WRF-HAILCAST model is 54 dBZ. This value has reached the minimum threshold for hail from [17], which is 52 dBZ. In addition, the presence of a high reflectivity value indicates that the number and size of the hydrometeor particles are increasing and getting bigger [18].

Fig. 2 shows a time series graph of the maximum reflectivity of the weather radar and the output of the WRF-HAILCAST model every 10 minutes. In the figure, it can be seen that the time of hail occurrence cannot be estimated

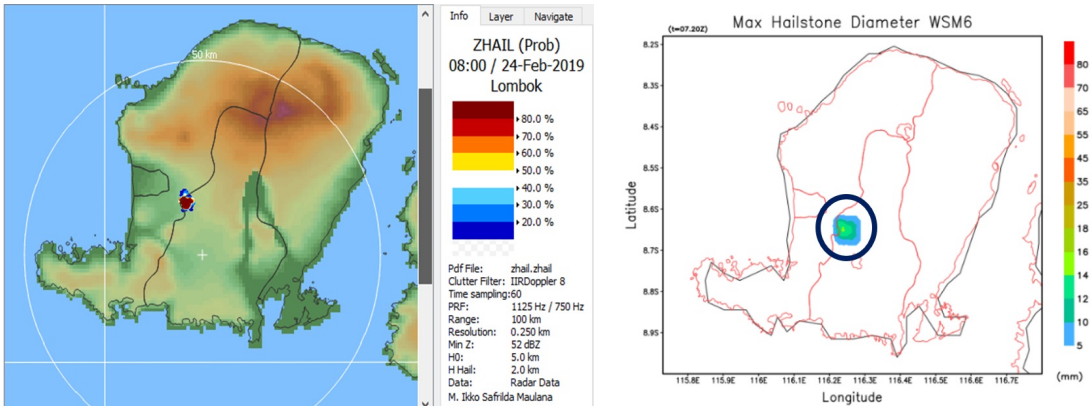

(a) (b)

FIG. 3: Hail location (based on ZHAIL product radar) and estimation of hailstone maximum diameter.

properly using WRF-HAILCAST. On the weather radar, hail can be detected with a maximum value of 61 dBZ at 08.00 UTC. While the output of the WRF-HAILCAST model shows the time of hail at 07.20 UTC. The difference in the time of hail occurrence can be influenced by several factors were hail growing from cloud systems with low reflectivity and small scale (less than 1 km). Furthermore, estimating the reflectivity value from the model is difficult because the reflectivity value depends on the mixing ratio and distribution of precipitation particles, but the model output may be able to produce a fairly good precipitation process [17]. So that it could not be represented properly in this study. To improve the models timing accuracy it can be done by increasing the resolution of the model (1 km resolution or finer), extending the time-step model of more than 12 hours, because the time-step model is very influential on the stable conditions in the modeling, and choosing the right microphysical scheme in the region.

B. Hailstone Maximum Diameter Distribution and Cloud Vertical Profile

The results of the distribution and estimation of hailstone size using weather radar and WRF-HAILCAST were presented in Fig. 3. Using the average criterion for the tropics, which was the height of freezing level at an altitude layer of 5 km, or around 560 mb, there was a potential of >80% of hail in Central Lombok at 08.00 UTC. As a result, it can be used as a verifier for the location of hail occurrence. This ZHAIL product can reflect the possibility for hail to occur, which is quite high (more than 80% probability).

The largest hailstone produced by WRF-HAILCAST had a maximum diameter distribution of 16 mm or 1.6 cm. Due to the lack of data for measuring the hailstone's diameter at the time of the incidence, the results of the estimation of the hailstone's diameter could not be confirmed with observational data. So, to verify the output of the WRF-HAILCAST model, it is important to measure in situ hailstone during hail storms in Indonesia. Furthermore, assuming the area of hail from ZHAIL products was the actual location. The hail location from the model showed the near of actual location. So, this modified model could simulate the hail location properly.

The WRF-HAILCAST output could properly represent the vertical structure of the cloud based on the vertical reflectivity of the cloud, however, the time of occurrence did not match the observations. This was shown by a vertical reflectivity pattern that was essentially identical to VCUT products, but the model's estimate of vertical velocity in the 7-8 km layer was 5060 dBZ, which was higher than the radar's estimate of 5055 dBZ (Radar observation), as shown in Fig. 4. The existence of a strong reflectivity pattern above the freezing level layer allows hail to occur because small hailstone particles were concentrated above the freezing level layer and could be lifted to the top layer during an updraft [19].

The vertical velocity pattern showed (in black line contour) -0.6 m/s until -1.8 m/s at 1000-400 mb layer during hail event. This value showed there was downdraft during hail. The presence of downdraft could enhance the hail reach surface [20]. But this variable could not be verified by the radar data because there was no data in v-component radar at the 45°-90° elevation. So that this variable could be represented by the model properly although there was no observation data.

C. Hail-Producing Cloud Microphysics

To ascertain the concentration of hydrometeor particles contained in the cloud during the hail occurrence, an examination of the microphysics process of hail-producing clouds was conducted. Utilizing the mixing ratio of each type of hydrometeor, this analysis was conducted. Water vapor (QVAPOR), cloud water (QCLOUD), rainwater (QRAIN), ice (QICE), and graupel are the types of hydrometeor particles examined in this study (QGRAUP). The outcomes for each type of hydrometeor particle are shown in Fig. 5.

The graph depicts the water vapor particle concentration from the 950 mb layer to the 200 mb layer. Above the layer of the freezing point, the highest concentration of water vapor particles is between 6.2 and 0.3 g/kg. The spontaneous rime process, which occurs when water vapor transforms directly

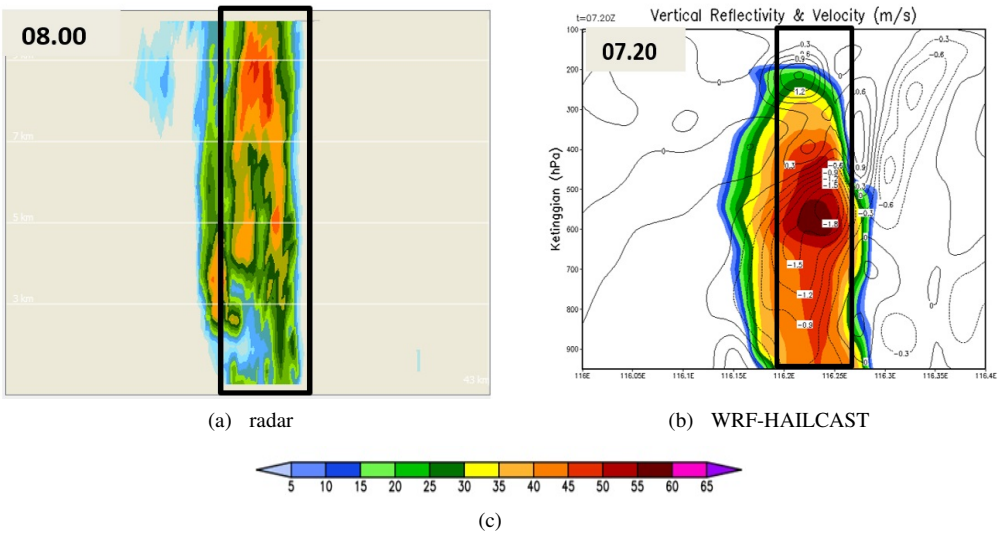

(a) radar (b) WRF-HAILCAST

(c)

FIG. 4: Vertical reflectivity at the time of hail event from (a) radar and (b) WRF-HAILCAST.

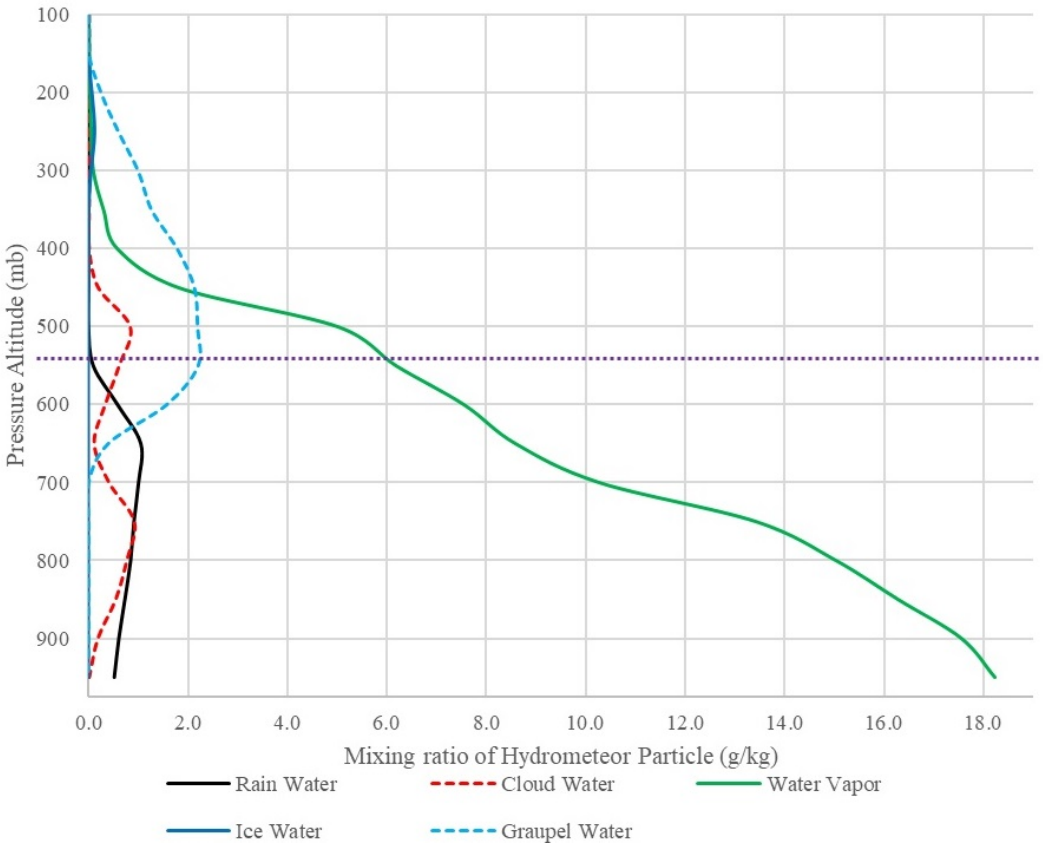

FIG. 5: Microphysics of cloud vertically at the time of hail occurrence

into ice or ice nuclei without first going through the liquid phase, was made possible by the presence of water vapor particles at a height above the freezing level layer [21]. A phase transition of the cloud water particles into supercooled water was produced at the below-freezing level which was 0.3 g/kg. A minimum of 0.1 g/kg of ice particles are also present in the 250 mb layer that was indicated the ice particles are still being lifted from the layer 450-250 mb which was supported by the updraft 0.3-0.6 m/s in Fig. 4. The presence of ice particles in this relatively high layer suggests that it has

a minor role in the production and growth of hail in clouds [22].

When clouds are carried higher by an updraft, the process of graupel production and growth happens from supercooled water [23]. Layers between 700 and 150 mb showed graupel mixing ratio values, with a maximum value of 2.2 g/kg. Indicating a successful merging and formation process where cloud water particles could develop and transform into rainwater and rain water could influence graupel forming. As shown by graupel water (blue dot line), the graupel particles were present at the same height and above cloud water particles (600-500 mb). Meanwhile, the fact that there are graupel particles beneath the freezing level layer suggests that the hail was small and had a chance of reaching the surface because it continues to exist after passing through the layer [3].

Furthermore, layers in the level from 950 mb to 400 mb contained rainwater droplets. Between a layer of 950 mb and 500 mb, the maximum value of rainwater particles varies from 0.1-1.0 g/kg. Particles of rainwater were found above the layer of the freezing level, indicating that the rainwater had undergone supercooling process [19]. Ice or hail formation is profoundly influenced by the presence of supercooled water [24, 25]. Graupel particles and or small hail will form when supercooled water collides and coalesces with ice particles under these conditions.

IV. CONCLUSION

Based on the results of the research that has been done, it can be concluded that WRF-HAILCAST with this modification of the WSM6 microphysical scheme can detect the presence of hail. The maximum reflectivity value near the surface produced by WRF-HAILCAST tends to be underestimated compared to the maximum reflectivity of radar. Meanwhile, the hail time occurrence in WRF-HAILCAST cannot estimate the time of occurrence according to the radar. There is a lag time of about 40 minutes between the WRF-HAILCAST results and the weather radar where the hail produced by WRF-HAILCAST precedes. The vertical profiles and microphysics process of the cloud can be simulated properly. The suggestions of the next research to improve the time accuracy in the model are increasing resolution up to 1 km or finer, extending the time-step model, and choosing the right microphysical scheme in Indonesia region. This model can contribute to hailstone detection in Indonesia using numerical method and give a breakthrough in hailstone detection and disaster preparedness.

Acknowledgments

The author would like to thank those who have assisted in the preparation of this journal until it is completed properly, namely the National Research and Innovation Agency (BRIN) which has lent access to High Performance Computing (HPC) for processing the WRF-HAILCAST numerical model, Head Climatological Station of West Lombok and Meteorological Station of Zaenuddin Abdul Madjid who have assisted in the data request process.

[1] BMKG, "Regulation of the Head of BMKG Number Kep. 009 of 2010 concerning Standard Operating Procedures for Implementation of Early Warning, Reporting, and Dissemination of Extreme Weather Information", Jakarta: BMKG, 2010.
[2] W.-K. Tao, *et al.*, "High-Resolution NU-WRF Simulations Of A Deep Convective-Precipitation System During MC3E: Further Improvements And Comparisons Between Goddard Microphysics Schemes And Observations", J. Geophys. Res. Atmos., vol. 121, pp. 12781305, 2016.
[3] M. Rajeevan, *et al.*, "Sensitivity of WRF cloud microphysics to simulations of a severe thunderstorm event over Southeast India", Ann. Geophys., vol. 28, pp. 603619, 2010.
[4] A. Fadholi, "Analisa Kondisi Atmosfer pada Kejadian Cuaca Ekstrem Hujan Es (Hail)", SIMETRI: Jurnal Ilmu Fisika Indonesia, vol. 1, no.2D, pp. 74-80, 2012.
[5] J.C. Brimelow, G.W. Reuter, and E.R. Poolman., "Modeling maximum hail size in Alberta thunderstorms", Wea. Forecasting, vol. 17, pp. 10481062, 2002.
[6] R.D. Adams-selin, and C.L. Ziegler, "Forecasting Hail Using a One Dimensional Hail Growth Model within WRF", Mon. Weather Rev., vol. 144, pp. 4919-4939, 2016.
[7] M.L. Weisman, W.C. Skamarock, and J.B. Klemp, "The resolution dependence of explicitly modeled convective systems", Mon. Wea. Rev., vol. 125, pp. 527548, 1997.
[8] J.S. Kain, *et al.*, "Examination of convection-allowing configurations of the WRF model for the prediction of severe convective weather: The SPC/NSSL Spring Program 2004", Wea. Forecasting, vol. 21, pp. 167181, 2006.
[9] C.A.D Permata, "Modifikasi Metode Waldvogel Berdasarkan Identifikasi Karakteristik Hujan Es di Wilayah Jawa Bagian Barat", Thesis, Sekolah Tinggi Meteorologi Klimatologi dan Geofisika, Tangerang, Indonesia, 2018.
[10] M.S. Djakaria, "Uji Sensitivitas Skema Parameterisasi Mikrofisik dengan Verifikasi Radar Cuaca untuk Simulasi Fenomena Hujan Es (Studi Kasus: Jakarta, 22 November 2018)", Buletin GAW Bariri, vol. 1, no. 2, pp. 94-100, 2020.
[11] SELEX., "Software Manual Rainbow 5 Product & Algorithms", Germany: SELEX SIGmbH, 2013.
[12] G.N. Harris, K.P. Bowman, & D.B. Shin, "Comparison of Freezing-Level Altitudes from the NCEP Reanalysis with TRMM Precipitation Radar Brightband Data", Journal of Climate, vol. 13, no.23, pp. 4137-4148, 2000.
[13] H.R. Stanski, L.J. Wilson, and W.R. Burrows., "Survey of Common Verification Methods in Meteorology", World Weather

Watch Tech. Rept. No.8, WMO/TD No.358, Geneva: WMO, 1989.

[14] Sudjana, "Teknik Analisis Regresi dan Korelasi", Bandung: Tarsito, 1996.

[15] Sugiyono, "Statistika untuk Penelitian",Bandung: Alfabeta, 2004.

[16] CAWCR., "Introduction of Verification Methods", URL: https://www.cawcr.gov.au/projects/verification, 2015.

[17] K.H. Min, *et al.*, "Evaluation of WRF Cloud Microphysics Schemes Using Radar Observations", Weather and Forecasting, vol. 30, no. 6, pp. 1571-1589, 2015.

[18] J.M. Wallace. and P.V. Hobbs, "Atmospheric Science: An Introductory Survey", Elsevier, pp. 92, 2006.

[19] G.G. Wisnawa, *et al.*, "Pemanfaatan Model WRF-ARW untuk Simulasi Hujan Sangat Lebat di Bandara I Gusti Ngurah Rai Bali (Studi Kasus Tanggal 12 Januari 2019)", Prosiding Seminar Nasional Fisika dan Pendidikan Fisika 2019, Universitas Yogyakarta, pp. 56-53, 2019.

[20] F.P. Sari, A.P. Baskoro, and O.S. Hakim, "Effect of Different Microphysics Scheme on WRF Model: A Simulation of Hail Event Study Case in Surabaya, Indonesia", AIP Conference Proceedings, vol. 1987(1):020002, July 2018, DOI: 10.1063/1.5047287.

[21] C.D. Ahrens, "Meteorology Today an Introduction to Weather, Climate and the Environment", USA: Cengage Learning, 2009.

[22] S. Zhang, S. Liu, and T. Zhang, "Analysis on the Evolution and Microphysical Characteristics of Two Consecutive Hailstorms in Spring in Yunnan, China", Atmosphere, vol. 12, no. 1, pp. 63-82, 2021.

[23] D. Martnez-Castro, *et al.*, "The Impact of Microphysics Parameterization in the Simulation of Two Convective Rainfall Events over the Central Andes of Peru Using WRF-ARW", J. Atmosphere, vol. 10, no. 8, pp. 442, 2019.

[24] Tjasyono, Bayong, "Mikrofisika Awan dan Hujan", Jakarta: BMKG, 2012.

[25] S.Y. Hong, J. Dudhia, & S.H. Chen, "A revised approach to ice microphysical processes for the bulk parameterization of clouds and precipitation", Mon. Weather Rev., vol. 132, issue 1, p. 103120, 2004, DOI: https://doi.org/10.1175/1520-0493(2004)132¡0103:ARATIM¿2.0.CO;2.